

Stimulated Short-Wave Radiation due to Single-Frequency Resonances of $\chi^{(3)}$

A. Penzkofer, A. Laubereau, and W. Kaiser

Physik Department der Technischen Universität München, München, Germany

(Received 17 July 1973)

Single laser pulses at 9455 cm^{-1} can generate spectra out to $30\,000 \text{ cm}^{-1}$ without self-focusing. Experimental data for water are explained by primary and secondary stimulated four-photon processes.

Recently, processes involving resonant enhancement of the third-order nonlinear susceptibility $\chi^{(3)}$ have received increasing attention. Four-photon frequency mixing has been studied with optical transitions in crystals¹ and in gases.² In these investigations advantage is taken of the terms of $\chi^{(3)}$ which contain difference frequency resonances (Raman type).

In this Letter we report on the observation of intense short-wavelength radiation when a single pulse of picosecond duration traverses an isotropic medium. Single-frequency resonances of $\chi^{(3)}$ are responsible for the very high gain of the four-photon emission observed in the forward direction.³ This type of resonance has been neglected in the past on account of the large infrared absorption at the idler frequency. We believe that our data give the first quantitative comparison between a broad-band stimulated parametric process and the frequency dependence of $\chi^{(3)}$ due to various single (infrared) resonances of the material. In addition, our investigations shed new light on the problem of "superbroadening" discussed recently by several authors.⁴

In this note we concentrate on investigations of water.⁵ Water was chosen for the following reasons: (i) The gain for stimulated Raman scattering is small in water⁶; single resonant processes are studied without appreciable contribution of Raman susceptibilities. (ii) The nonlinear index of refraction n_2 of water⁷ is known to be small. In this way the threshold for self-focusing is high ($I_{\text{th}} > 10^{12} \text{ W/cm}^2$ in our investigations) and the frequency broadening due to self-phase modulation⁸ is negligible ($\Delta\nu \approx 6 \text{ cm}^{-1}$ at 10^{11} W/cm^2).

In our experiments single pulses were cut from trains of a mode-locked Nd-glass laser.⁹ The single pulses have a duration of $\Delta t_L \approx 6 \text{ psec}$; they were bandwidth limited ($\Delta\nu_L \approx 3 \text{ cm}^{-1}$) with a peak intensity $I_{0L} \leq 1.5 \times 10^{11} \text{ W/cm}^2$. Investigations of the intensity distribution over the cross section of the laser beam were made at the exit window of the cell (length 2 cm); no effects due to self-focusing were observed at the input in-

intensities discussed here. Measurements of the angular distribution revealed that the short-wavelength radiation occurred in the forward direction with a small angle of divergence ($2\theta \approx 4 \times 10^{-2}$ rad). The polarization of the generated radiation was found to be parallel to the polarization of the laser light. Qualitative information of the emission was obtained with spectrographs. A more detailed study of the spectra was made with a double monochromator (wavelength resolution 33 Å) in conjunction with calibrated photomultipliers. The energy conversion per frequency interval was measured as a function of input peak intensity I_{0L} for forty frequencies. As an example, experimental data are presented for three frequencies in Fig. 1. Two points should be noted here: First, the rapid rise in energy conversion of 7 orders of magnitude within a small in-

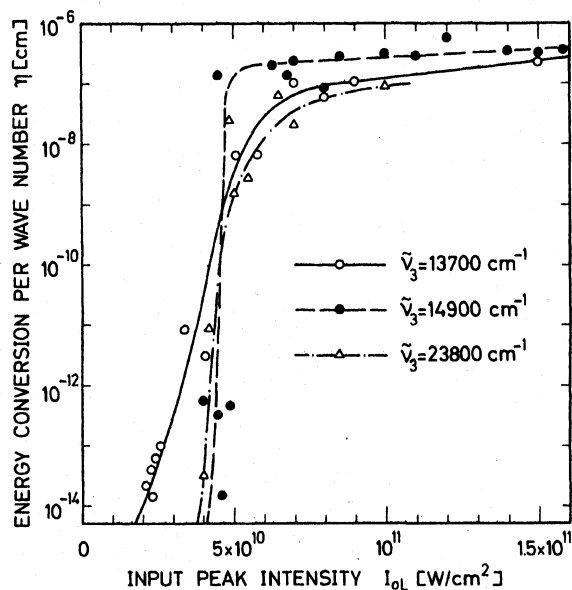


FIG. 1. Energy conversion η of laser emission ($\tilde{\nu}_L = 9455 \text{ cm}^{-1}$) into short-wavelength radiation at $\tilde{\nu}_3$. The curves below $\eta = 10^{-8}$ are calculated for $\tilde{\nu}_3 = 13\,700$ and $14\,900 \text{ cm}^{-1}$ with $\chi^{(3)}$ values taken from Fig. 4.

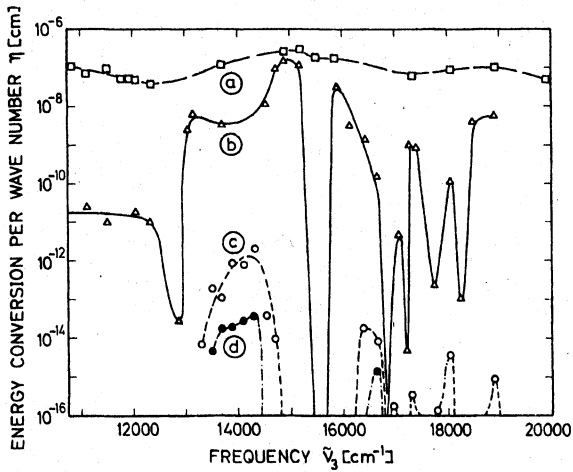


FIG. 2. Experimental energy conversion η versus signal frequency $\tilde{\nu}_3$ for four laser input peak intensities: a, 1×10^{11} ; b, 5×10^{10} ; c, 3×10^{10} ; d, 2×10^{10} W/cm 2 .

terval of input intensity; the situation is most drastic for $\nu_3 = 14900 \text{ cm}^{-1}$, indicating an amplification process of large gain. Second, at input peak intensities exceeding $5 \times 10^{10} \text{ W/cm}^2$ the energy conversion saturates with similar values for the three frequencies. In Fig. 2 the energy conversion is depicted over the frequency range from 10800 to 20000 cm^{-1} ; four curves for different input intensities are presented. For $I_{0L} \leq 5 \times 10^{10} \text{ W/cm}^2$ a striking structure of the spectra is clearly visible. These spectra and their input dependence can be explained by the single-photon resonance structure of $\chi^{(3)}(-\omega_3, \omega_L, \omega_L, -\omega_4)$ of water. The flat spectrum at $I_{0L} \approx 10^{11} \text{ W/cm}^2$ extends out to 30000 cm^{-1} ; it is determined by saturation effects in the center of the beam and by secondary parametric processes (see below).

For a quantitative explanation of our observations we have calculated the stimulated parametric four-photon interaction for very general conditions: finite bandwidth $\Delta\omega$ of the pump pulses, phase mismatch $\Delta k = k_1 + k_2 - k_3 - k_4$, and absorption at signal and idler frequencies of α_3 and α_4 , respectively. In Eq. (1) the quantities Δk , α_3 , α_4 , and $\chi^{(3)}(-\omega_3, \omega_1, \omega_2, -\omega_4)$ and the spectral intensities $\epsilon(\omega_3, z)$ and $\epsilon(\omega_4, z)$ (energy per cross section and wave number) are average values over $\Delta\omega$. Assuming no depletion of the pump we find¹⁰

$$\epsilon(\omega_3, z) = \epsilon_4 |\sinh \gamma z|^2 \frac{G |\chi|^2 \omega_3}{4 |\gamma|^2 \omega_4} e^{-\alpha z}, \quad (1)$$

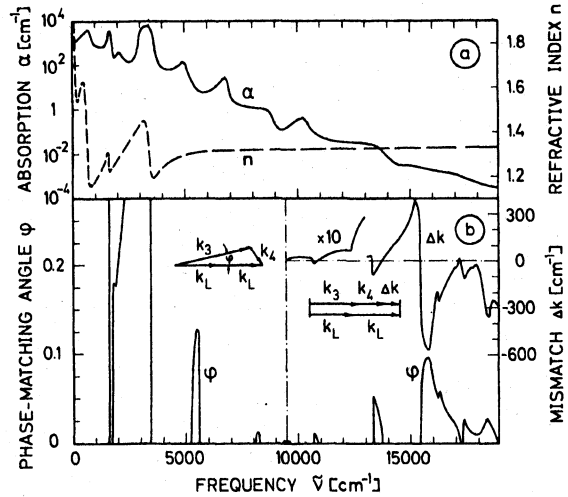


FIG. 3. (a) Absorption coefficient α (Ref. 12) and refractive index n of water. (b) Noncollinear phase-matching angle ϕ (rad) and collinear phase mismatch Δk for the interaction $\omega_L + \omega_L \rightarrow \omega_3 + \omega_4$.

where

$$G = \frac{1024 \pi^4 \omega_3 \omega_4 I_{01}(z) I_{02}(z)}{n_1 n_2 n_3 n_4 c^4},$$

$$\gamma = 0.25 [\alpha_d^2 + 4(G\chi^2 - \Delta k^2 + i\Delta k \alpha_d)]^{1/2},$$

$$\chi = \chi_{xxxx}^{(3)}(-\omega_3, \omega_1, \omega_2, -\omega_4) = \chi' + i\chi'';$$

I_{01} and I_{02} are the peak intensities of the pump pulses centered at ω_1 and ω_2 . $\alpha = (\alpha_3 + \alpha_4)/2$, $\alpha_d = \alpha_4 - \alpha_3$, and $\epsilon_4 = \epsilon(\omega_4, 0)$.

In the primary parametric process we have $\omega_L + \omega_L \rightarrow \omega_3 + \omega_4$. The initial conditions are $\epsilon(\omega_3, 0) = 0$ for the signal and quantum noise for the idler¹¹ (primary process). According to Fig. 3(a) the absorption coefficient¹² is small at the signal frequencies $\omega_3 > \omega_L$ but very large for certain idler frequencies ω_4 . Figure 3(b) illustrates the phase-matching situation. Large phase-matching angles are required for $\Delta k = 0$ over a considerable part of the spectrum. (Note the large walk-off angle of the idler.) Experimentally, the short-wave radiation was found within a small angle in the forward direction. As a result, we have to consider a (collinear) mismatch Δk over a considerable frequency range. Fortunately, the large values of $\chi^{(3)}$ and of I_{0L} make strong amplification possible in spite of substantial values of Δk and α_4 .¹³

The nonlinear susceptibility $\chi^{(3)}$ consists of terms with single- and difference-frequency (Raman-type) resonance denominators.^{14,15} $\chi'' = \chi_I''$

χ_R'' and $\chi' = D\chi_{NR} + \chi_I' + \chi_R'$ are written as follows:

$$\chi'' = K \sum_i \langle g | x | c_i \rangle \langle c_i | x^3 | g \rangle \frac{\Gamma_{c_i}}{(\omega_{c_i} - \omega_4)^2 + \Gamma_{c_i}^2} + \sum_j \chi_{R,j}'' \quad (2)$$

$$\chi' = D\chi_{NR} + \sum_i \chi_{I,i}' \frac{\omega_{c_i} - \omega_4}{\Gamma_{c_i}} + \sum_j \chi_{R,j}' \left(\frac{\omega_{b_j} - \omega_1 + \omega_4}{\Gamma_{b_j}} + \frac{\omega_{b_j} - \omega_2 + \omega_4}{\Gamma_{b_j}} \right) \quad (3)$$

where $|g\rangle$ and $|c_i\rangle, |b_j\rangle$ denote the ground and excited states of the material, respectively; ω_{c_i} and ω_{b_j} are the corresponding resonance frequencies, and Γ_{c_i} and Γ_{b_j} are the half-widths of the resonances. The small frequency dependence of the quantity K is neglected in our calculations. D is 6 for $\omega_1 \neq \omega_2$ and 3 for $\omega_1 = \omega_2$. The nonresonant term¹⁵ χ_{NR} and the Raman terms⁶ χ_R'' have been the subject of previous investigations. The frequency-dependent $\chi_I''(-\omega_3, \omega_1, \omega_2, -\omega_4)$ is taken to be proportional to the absorption spectrum $\alpha(\omega_4)$ by assuming $\langle c_i | x^3 | g \rangle$ to be proportional to $\langle c_i | x | g \rangle$.¹⁶ Knowing the absolute values of χ_{NR} , χ_R'' , and χ_R' [Eq. (3)], the relative frequency dependence of χ_I'' , and the relation between χ_I'' and χ_I' [Eq. (3)], we calculated the absolute values of χ_I'' and χ_I' using experimental data around $\tilde{\nu}_3 = 15000 \text{ cm}^{-1}$ [Eq. (1)]. Because of several ap-

proximations in the calculation of χ , the absolute values may be accurate within a factor of 2 only. In Fig. 4(a) we present χ_R'' and χ_I'' and in Fig. 4(b), $\chi' = 3\chi_{NR} + \chi_I' + \chi_R'$. The points in Fig. 4(b) correspond to the experimental data of Fig. 2 ($I_{OL} \leq 5 \times 10^{10}$). Note the good agreement between experiment and the frequency dependence of χ' over a frequency range of 8000 cm^{-1} . In particular, the minima in the energy-conversion curves in Fig. 2 are fully accounted for by the maxima of χ_I'' at $\tilde{\nu}_3 = 18250, 17250,$ and 15600 cm^{-1} ($\chi' \approx 0$) and by the change in sign of χ_I' at $\tilde{\nu}_3 = 17650$ and 16800 cm^{-1} . We feel that this result is convincing evidence for the importance of single-frequency resonances of $\chi^{(3)}$. It is interesting to see the effect of the Raman susceptibility at 12900 cm^{-1} , where a minimum is observed in Fig. 2 (inverse Raman effect).

In Fig. 2 the energy conversion for $I_{OL} > 5 \times 10^{10} \text{ W/cm}^2$ is found to be $\eta \approx 2 \times 10^{-7} / \text{cm}^{-1}$. Considering the large spectral range of approximately 25000 cm^{-1} we estimate a total energy conversion of $\eta_{tot} \approx 5 \times 10^{-3}$. On account of the large gain values observed in Fig. 1, the energy conversion will be large where I_L is high, i.e., in the center of the pulse. Calculations indicate that only approximately one fifth of the beam diameter contributes to the radiation at ω_3 when η approaches saturation. Under these conditions the peak intensity of the generated radiation ($I_{O2} \approx \eta_{tot} I_{OL} d_L^2 \Delta t_L / d_2^2 \Delta t_2$) is of the same magnitude as I_{OL} .

The intense light pulse discussed above acts as a broad-band pump (ω_2) for secondary processes of the form $\omega_L + \omega_2 = \omega_3 + \omega_4$.¹⁷ Very short frequencies at $\omega_3 > 2\omega_L$ are generated ($\omega_2 > \omega_L, \omega_4 < \omega_L$) and frequency components are produced which smooth the spectral distribution of the primary process (e.g., at minima of Fig. 2). As a brief example we consider the energy conversion at $\tilde{\nu}_3 = 23800 \text{ cm}^{-1}$ (see Fig. 1). For the frequency range of $\tilde{\nu}_2$ between 14400 and 18900 cm^{-1} and with $I_{OL} = 5 \times 10^{10} \text{ W/cm}^2$ and $I_{O2} \approx 10^{-2} I_{OL}$, we find $\eta \approx 10^{-10}$ to $10^{-9} / \text{cm}^{-1}$. This estimate shows that light generated in the secondary process can build up to values found in the primary process.

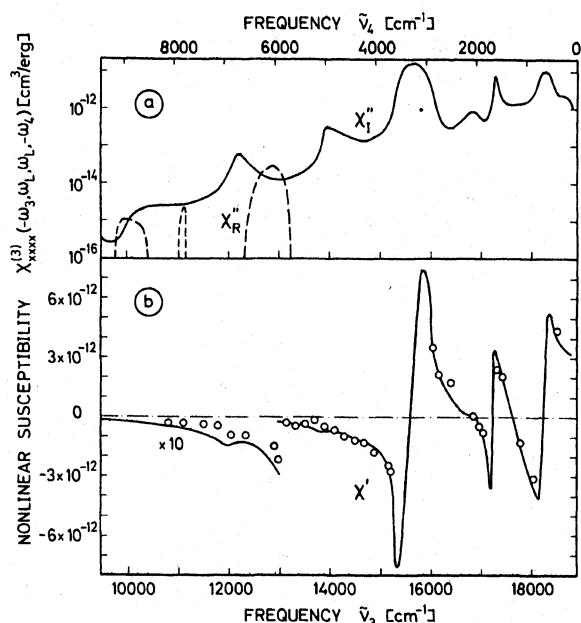


FIG. 4. Nonlinear susceptibility $\chi^{(3)}$ of water. (a) Imaginary parts χ_I'' and χ_R'' ; χ_I'' is obtained from the absorption spectrum α . (b) Real part $\chi' = 3\chi_{NR} + \chi_I' + \chi_R'$ [$\chi_{NR} \approx 2 \times 10^{-14} \text{ cm}^3/\text{erg}$ (Ref. 15)]. The curve is calculated [Eq. (1)] by fitting to experimental data around $\tilde{\nu}_3 = 15000 \text{ cm}^{-1}$. Open circles, experimental points.

In summary, we have observed and explained broad short-wave radiation under well-defined experimental conditions. In our experiments, self-phase modulation is negligible and self-focusing is absent. It is expected—and preliminary experiments confirm—that the same physical mechanism contributes to superbroadening also in other materials under more complex experimental conditions.⁴

¹M. D. Levenson, C. Flytzanis, and N. Bloembergen, *Phys. Rev. B* **6**, 3962 (1972); J. J. Wynne and J. R. Lankard, *Appl. Phys. Lett.* **29**, 650 (1972).

²P. P. Sorokin, J. J. Wynne, and J. R. Lankard, *Appl. Phys. Lett.* **22**, 342 (1973).

³Noncollinear phase-matched four-photon interaction has been reported in self-focused beams by R. R. Alfano and S. L. Shapiro, *Phys. Rev. Lett.* **24**, 584 (1970).

⁴For references see S. A. Akhmanov, R. V. Khokhlov, and A. P. Sukhorukov, in *Laser Handbook*, edited by F. T. Arecchi and E. O. Schulz DuBois (North-Holland, Amsterdam, 1972).

⁵D. L. Weinberg, *Appl. Phys. Lett.* **14**, 32 (1969); W. Werncke, A. Lau, M. Pfeiffer, K. Lenz, H.-J. Weigmann, and C. D. Thuy, *Opt. Commun.* **4**, 413 (1972); V. S. Dneprovsky, K. V. Karmenjan, and I. I. Nurminsky, *Izv. Akad. Nauk Arm. SSR, Fiz.* **7**, 348 (1972).

⁶O. Rahn, M. Maier, and W. Kaiser, *Opt. Commun.* **1**, 109 (1969); G. E. Walrafen, *J. Chem. Phys.* **47**, 114 (1967), and private communication.

⁷M. Paillette, *Ann. Phys. (Paris)* **4**, 671 (1969).

⁸R. R. Alfano, L. L. Hope, and S. L. Shapiro, *Phys. Rev. A* **6**, 433 (1972).

⁹D. von der Linde, *IEEE J. Quant. Electron.* **8**, 328 (1972).

¹⁰As a guide for deriving Eq. (1) see A. Yariv and J. E. Paerson, in *Progress in Optics*, edited by J. H. Sanders and K. W. H. Stevens (Pergamon, New York, 1969), Vol. 1.

¹¹For a discussion of the initial conditions see Ref. 10, and A. Yariv, *Quantum Electronics* (Wiley, New York, 1968).

¹²E. K. Plyler and N. Acquista, *J. Opt. Soc. Amer.* **44**, 505 (1954).

¹³The group-velocity dispersion allows an interaction between pump $\tilde{\nu}_L$ and signal $\tilde{\nu}_s$ for more than 4 cm.

¹⁴J. A. Armstrong, N. Bloembergen, J. Ducuing, and P. S. Pershan, *Phys. Rev.* **127**, 1918 (1962).

¹⁵R. W. Terhune and P. D. Maker, in *Lasers*, edited by A. K. Levine (Marcel Dekker, New York, 1968), Vol. 2.

¹⁶This assumption may be justified as follows: $\langle c_i | x^3 | g \rangle = \sum_j \langle c_i | x | a_j \rangle \langle a_j | x^2 | g \rangle \approx \sum_j \langle c_i | x | a_j \rangle \langle a_j | x^2 | g \rangle = \langle c_i | x | \bar{a} \rangle \times \sum_j \langle a_j | x^2 | g \rangle = \langle c_i | x | \bar{a} \rangle C_1 \approx \langle c_i | x | g \rangle C_2$, C_1 and C_2 being constants. The first sum runs over all states $|a_j\rangle$ with the same parity as $|g\rangle$ (other matrix elements are zero). In the second sum only the states $|a_j\rangle$ are retained which form large matrix elements. These states $|a_j\rangle$ have a shape similar to $|g\rangle$. This fact implies that $|\bar{a}\rangle$ is similar to $|g\rangle$ in the averaged matrix element $\langle c_i | x | \bar{a} \rangle$ and that $\langle c_i | x | \bar{a} \rangle \approx \text{const} \times \langle c_i | x | g \rangle$.

¹⁷Preliminary calculations show that frequency conversion, $\omega_L + \omega_L + \omega_4 \rightarrow \omega_3$, contributes at high laser intensities.

Excitation of Quasicylindrical Waves Connected with Electron Bernstein Modes

A. Gonfalone

Space Science Department, European Space Research Organization, Noordwijk, Holland

and

C. Beghin

Groupe de Recherches Ionosphériques, Centre National de la Recherche Scientifique, 45045 Orléans, France

(Received 24 May 1973)

By measuring the potential around a point-source antenna in a high-density magnetoplasma at a frequency between the electron gyrofrequency and the plasma frequency, we have detected an interference between a slow electrostatic wave and the cold plasma field. A model of quasicylindrical electrostatic waves connected with the Bernstein mode is proposed to explain the results.

We have measured the potential around a small antenna embedded in a magnetoplasma. According to cold-plasma theory, the potential is maximum on a cone with its apex at the source and its axis along the magnetic field when the frequency

is either in the range of the upper oblique resonance (ω between the plasma frequency ω_p , or the gyrofrequency ω_c if $\omega_c < \omega_p$, and the upper-hybrid frequency) or in the range of the lower oblique resonances ($\omega < \omega_c$ or ω_p if $\omega_c > \omega_p$).